



Original Article

Computed tomography-guided frame-based stereotactic brain biopsy of non-enhancing lesions using indirect evidence of target selection, technical consideration, and early clinical experience

TS Lingaraju¹, AR Prabhuraj¹, BN Nandeesh², Jitender Saini³, Nupur Pruthi¹

Departments of ¹Neurosurgery, ²Neuropathology, ³NeuroImaging and Interventional Neuroradiology, NIMHANS, Bengaluru, Karnataka, India.

E-mail: *TS Lingaraju - drlingarajuts@gmail.com; AR Prabhuraj - drprabhuraj@yahoo.co.in; BN Nandeesh - nandeeshbn@gmail.com; Jitender Saini - jsaini76@gmail.com; Nupur Pruthi - pruthi_nupur@yahoo.co.in



***Corresponding author:**

TS Lingaraju,
Department of Neurosurgery,
NIMHANS, Bengaluru,
Karnataka, India.

drlingarajuts@gmail.com

Received: 15 March 2024

Accepted: 22 July 2024

Published: 16 August 2024

DOI

10.25259/SNI_187_2024

Quick Response Code:



ABSTRACT

Background: The objective was to study the effectiveness and diagnostic outcome of frame-based stereotactic brain biopsy (STB) done for contrast non-enhancing lesions using indirect evidence of target selection observed in a plain computed tomography (CT) scan of the head.

Methods: Data of patients with contrast non-enhancing brain lesions who underwent STB are collected retrospectively from NIMHANS Bangalore, hospital neurosurgery database from January 2021 to March 2023. Those cases subjected to plain CT scans after fixing the stereotactic frame to the head were included in the study. A final histopathological report analysis of these cases was done to assess the diagnostic accuracy.

Results: A total of 27 such cases were biopsied. The mean age of subjects was 44.04 ± 17.812 years. Most subjects were in the age group 31–40 years (29.6%). About 55.6% were male and 44.4% were female. The most common site of biopsy was the frontal lobe. The most common indirect evidence on CT was perilesional edema at 33.3% and periventricular location at 33.3%, followed by intralesional calcification at 11.1%. Our diagnostic accuracy was 92.59%. The asymptomatic hemorrhage rate was 2%, and an increase in perilesional edema was seen in 2% of cases.

Conclusion: Indirect targeting is a safe and intuitive method for biopsy of contrast non-enhancing lesions. Due consideration is to be given to various findings visible in non-contrast CT scans of the head as indirect evidence of target selection while performing frame-based STB of contrast non-enhancing lesions. This method will also be helpful in resource-limited centers, especially in low-income countries.

Keywords: Computed tomography scanning, Frameless stereo-tactic brain biopsy, Non-enhancing lesions

INTRODUCTION

Stereotactic brain biopsy (STB) is an invasive but safe diagnostic procedure performed to establish tissue/molecular diagnosis in various spectrums of diseases of the brain. Despite rapid advancement in brain imaging techniques, conventional histopathological, immunohistochemical, and molecular analysis remains the gold standard.^[1,5] The procedure aids in obtaining adequate brain tissue representative of the lesion and provides ample diagnostic

This is an open-access article distributed under the terms of the Creative Commons Attribution-Non Commercial-Share Alike 4.0 License, which allows others to remix, transform, and build upon the work non-commercially, as long as the author is credited and the new creations are licensed under the identical terms.

©2024 Published by Scientific Scholar on behalf of Surgical Neurology International

information for neuro-oncological treatment. At present, frame-based and frame-less STB techniques are in clinical use with non-inferiority of one over another.^[8] Traditional teaching is that while subjecting the patient to imaging after fixing the stereotactic frame, the same specific sequence of computed tomography (CT) or magnetic resonance imaging (MRI) scan should be done in which the lesion is better visualized. The enhancing lesion can thus be targeted accurately. The critical step in the frame-based technique is calculating stereotactic coordinates obtained by fusing a preoperative MRI image of the patient with a CT scan taken after fixing the stereotactic frame^[5] or from contrast-enhanced T1-weighted MRI/CT.^[12]

The problem we are trying to address is selecting a suitable target for a non-enhancing lesion. In such a case, target selection often becomes difficult, such as in the highly eloquent location of low-grade gliomas, resolving/incipient infections, recurrent gliomas, and radiation necrosis, leading to sampling errors.^[4] Various adjuncts of imaging, such as positron emission tomography (PET), magnetic resonance perfusion, and magnetic resonance spectroscopy, to help target selection have been published in the literature to address this issue.^[5] Using such adjuncts of imaging for mere target selection in case of non-enhancing lesions like low-grade gliomas is time-consuming and increases the cost of the procedure. Thus, we sought a novel targeting method to perform diagnostic STB in non-enhancing lesions without needing higher-order imaging. This method will also be helpful in resource-limited centers, especially in low-income countries. The authors propose a simple method for target selection of such lesions in appropriately selected cases using indirect evidence of target localization during CT-guided frame-based STB.^[2,4,7,9,10]

MATERIALS AND METHODS

This study is a retrospective review of clinical, imaging, and histopathological report data of patients with contrast non-enhancing intracranial space-occupying lesions who underwent frame (Leksell system) based stereotactic biopsy in our hospital. As it was a retrospective study of data from histopathological reports and a picture archival communication system, approval from our Institute's Ethical Committee was not sought. The appropriate case selection for the proposed new method was decided by careful study of preoperative radiological imaging. Imaging prerequisites for case selection are listed below.

- Lesion should be non-contrast enhancing (for example, low-grade gliomas) and
- Lesion exerting mass effect/midline shift [Figure 1] distorting surrounding brain normal anatomy such as effacement of adjacent gyri/sulci and obliteration of ventricle [Figure 2]

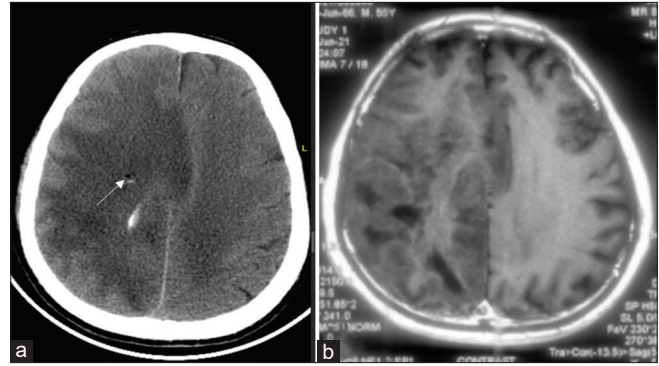


Figure 1: (a) Post procedure plain computed tomography showing midline shift and edema as an indirect evidence at corresponding cuts with a white arrow indicating biopsy site. (b) In an index case of the right diffuse hemispheric glioma preoperative contrast magnetic resonance imaging sequence.

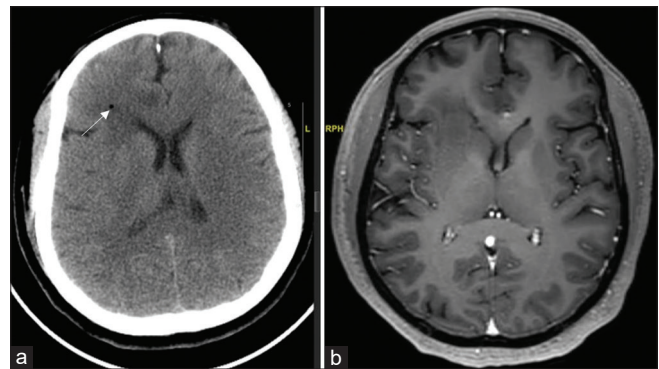


Figure 2: (a) Post procedure plain computed tomography showing right frontal periventricular location in relation to the caudate nucleus as an indirect evidence at corresponding cuts with white arrow indicating biopsy site. (b) In an index case of the right frontal glioma, preoperative contrast magnetic resonance imaging sequence.

- Lesion location about identifiable subcortical structures such as internal capsule [Figure 3]
- Lesion causing radiologically appreciable perilesional edema [Figure 4]
- Lesion with calcification [Figure 5].

Using this indirect evidence, most non-enhancing lesions can be precisely localized using non-contrast CT-based planning of target selection and coordinates calculation while performing frame-based STB.

Statistical analysis and software

Data were entered into a Microsoft Excel data sheet and were analyzed using the Statistical Package for the Social Sciences (SPSS) 22 version software. Categorical data were represented in the form of frequencies and proportions. Microsoft Excel and SPSS version 22 (IBM SPSS Statistics, Somers, NY, USA) were used to analyze data.

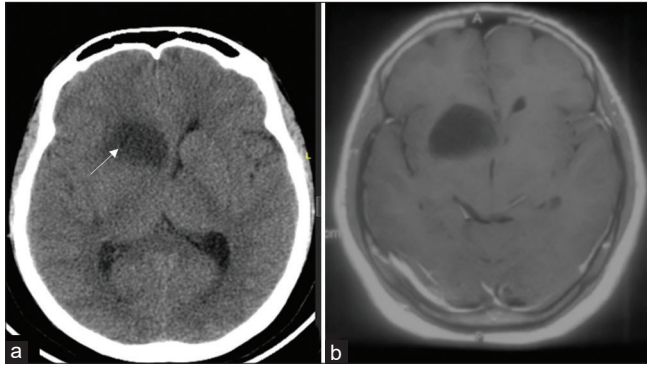


Figure 3: (a) Post procedure plain computed tomography showing lesion location in relation to the anterior limb of right internal capsule as an indirect evidence at corresponding cuts with white arrow indicating biopsy site. (b) In an index case of the right caudate glioma, preoperative contrast magnetic resonance imaging sequence.

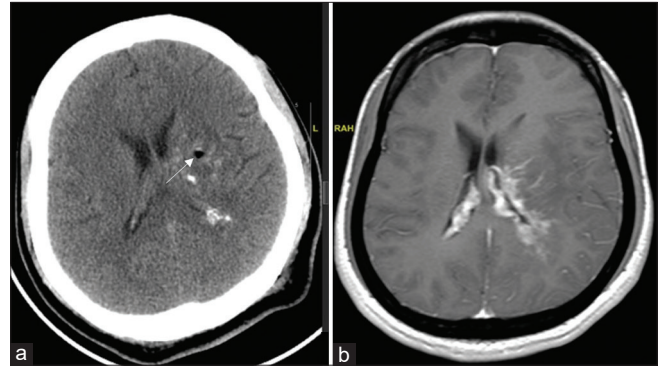


Figure 5: (a) Post procedure plain computed tomography showing intralesional calcification as an indirect evidence at corresponding cuts with a white arrow indicating the biopsy site. (b) In an index case of left thalamocapsular glioma preoperative contrast magnetic resonance imaging sequence.

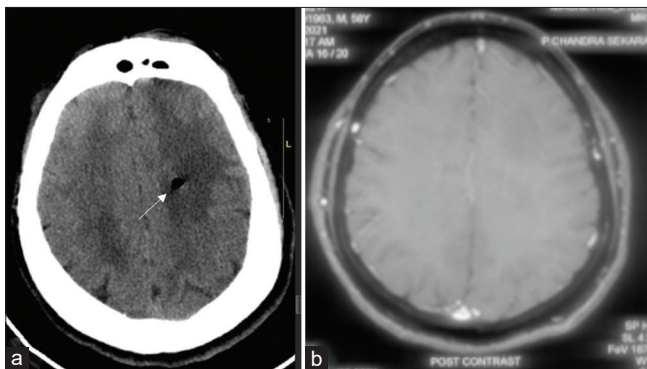


Figure 4: (a) Post procedure plain computed tomography showing mass effect and perilesional edema as an indirect evidence at corresponding cuts with white arrow indicating biopsy site. (b) In an index case of left diffuse hemispheric glioma preoperative contrast magnetic resonance imaging sequence.

Description of the procedure

Our institute uses the Leksell system for frame-based STB. All patients underwent contrast MRI preoperatively. On the day of surgery, the radiological images of suitable cases for this new target localization method were studied before starting the procedure. Using aseptic and antiseptic precautions, the Leksell frame was fixed to the patient's head with two pins in the frontal and two pins in the occipital region under local infiltration of lignocaine at pin sites. All patients underwent a 0.65 mm thin slice plain CT scan with the Leksell stereotactic frame fixed to their heads. We used indirect evidence of non-contrast CT for target localization as illustrated case by case. The target's stereotactic calculus was planned using MNPS software (Mevis, Sao Paulo SP, Brazil).

The frame center is given the numerical No 100, with the X-axis running horizontally using a grid at the CT scanner console and the Y-axis running vertically. The target coordinates are

determined based on this numerical No 100. The fiducial distance recorded in the CT console suggests the Z coordinate of the superoinferior stereotactic plane. We prefer to begin by taking a biopsy sample from the edge of the lesion and then moving to the center to avoid a negative biopsy. All parameters were calculated and then manually applied to the Leksell frame system. The trajectory was planned from the right or left frontal whenever possible to avoid eloquent structures.

Shaving and disinfection of 2–3 cm scalp over the planned entry point was performed. A small stab incision was placed over the entry point in the scalp after local infiltration of adrenaline and lignocaine. Twist drill trephination is done till the tip crosses the inner table of the skull, with the twist drill tip plunging across the dura. Tissue samples were taken with a Sedan biopsy needle (Micromar, Diadema SP, Brazil), which generates samples of 5 mm. Three samples were collected from the lesion margin before hitting the target. Another three samples were collected from the selected target site. After adequate tissue samples, the biopsy forceps were drawn back, and the skin was closed. The frame was detached from the head. We do postoperative CT scans routinely after 4 hours of the procedure for all the patients in our institute to confirm the biopsy track and to rule out intracerebral bleeding. The patients were kept in the recovery room and discharged home the same day.

RESULTS

The types of cases and indirect evidence can vary. From January 2021 to March 2023, 27 such cases were biopsied. The mean age of subjects was 44.04 ± 17.812 years. Most subjects were in the age group 31–40 years (29.6%), 55.6% were male, and 44.4% were female [Table 1]. The most common biopsy site was the frontal lobe [Table 2]. The most common indirect evidence of CT was perilesional edema in 33.3%, periventricular location in 33.3%, and intralesional

calcification in 11.1 % of the cases [Table 3]. Our diagnostic accuracy was seen in 25 cases (92.59 %), an inconclusive

Table 1: Patient characteristics among biopsy cohort (n=27).

	Count	Percentage
Age		
<20 years	3	11.1
21–30 years	2	7.4
31–40 years	8	29.6
41–50 years	5	18.5
51–60 years	4	14.8
>60 years	5	18.5
Gender		
Female	12	44.4
Male	15	55.6

Table 2: Spectrum of cases that underwent the procedure (n=27).

Clinical diagnosis	Count	Percentage
Gliomatosis cerebri	1	3.7
Corpus callosal glioma	2	7.4
Frontotemporal glioma	1	3.7
Left atrial glioma	1	3.7
Left frontal glioma	1	3.7
Left parieto-occipital glioma	1	3.7
Left posterior frontal lesion	1	3.7
Brain abscess	2	7.4
Left thalamic tumor	2	7.4
Low grade glioma	1	3.7
CNS lymphoma	4	14.8
Right frontal diffuse glioma	2	7.4
Right frontal lesion	1	3.7
Right frontal tuberculoma	1	3.7
Right frontal white matter disease	1	3.7
CNS toxoplasmosis	1	3.7
White matter disease	1	3.7
Right parietal glioma (post RT)	1	3.7

CNS: Central nervous system

Table 3: Analysis of indirect evidence in non-contrast CT observed during stereotactic brain biopsies (n=27).

Indirect evidence on non-contrast CT	Count	Percentage
Perilesional edema	9	33.3
Periventricular location	9	33.3
Intralesional calcification	6	22.2
Intraventricular location	1	3.7
Mass effect	2	7.4
Midline shift, edema	1	3.7
Anterior limb of internal capsule	1	3.7
Effacement of ipsilateral lateral ventricle	1	3.7
Splenium of corpus callosum	1	3.7
Total	27	100.0

CT: Computed tomography

histopathological diagnosis was reported in 2 cases (7.4 %), and none of the cases biopsy was negative [Tables 4-6]. The asymptomatic hemorrhage rate was 2%, and an increase in

Table 4: Histopathological diagnosis of the biopsies of 27 patients with non-contrast enhancing brain lesions/pathologies (n=27).

Histopathology findings	Count	Percentage
Astrocytoma, NOS, CNS WHO grade 3; splenial	1	3.7
Diffuse glioma	1	3.7
Diffuse glioma, NOS, WHO grade II,	1	3.7
Diffuse large B-cell lymphoma, right capsuloganglionic	2	7.4
Diffuse midline glioma WHO grade IV	1	3.7
Diffuse midline glioma, H3K27M mutant, CNS WHO grade 4, left thalamopeduncular	1	3.7
Fragments of neuroparenchyma with hemorrhage (? significance) and reactive changes, right frontal	1	3.7
GBM NOS WHO gr IV left frontal	1	3.7
Glioblastoma, NOS, IDH1 p.R132H negative by IHC, CNS WHO grade 4; corpus callosum	1	3.7
High grade glioma IDH mutant	1	3.7
High grade glioma (astrocytic phenotype), CNS WHO grade 3, right frontal	1	3.7
IDH mutant glioma	1	3.7
In view of an occasional MIB1 labeled cell, an adjacent/peripheral portion of a glial neoplasm cannot be excluded.	1	3.7
Inconclusive	2	7.4
Inflammatory pathology, favoring a Demyelinating etiology;	1	3.7
Left occipital granulomatous angiitis	1	3.7
Lymphoproliferative disorder, Left capsuloganglionic region	1	3.7
No diagnostic pathology, right frontotemporal	1	3.7
No distinct neoplasm identified	1	3.7
Oligodendroglioma, NOS, CNS WHO grade 3, Left frontal	1	3.7
Oligodendroglioma, NOS, WHO grade II, left parietal and occipital	1	3.7
Organizing pyogenic abscess wall	1	3.7
Radiation induced changes with few neoplastic cells	1	3.7
Reactive changes with focal necrosis; stereotactic biopsy	1	3.7
Comment: There is no overt evidence of lymphoma. Biopsy may not be representative.		
STB was not done as the lesion regressed with antibiotics	1	3.7
Total	27	100.0

CNS: Central nervous system, WHO: World Health Organization, GBM: Glioblastoma, IDH 1: Isocitrate dehydrogenase 1, IHC: Immunohistochemistry, NOC: Not Otherwise Specified, MIB1: antibody Mindbomb Homolog-1, STB: Stereo tactic brain biopsy

Table 5: Immunohistochemistry analysis (n=27).

Immunohistochemistry	Count	Percentage
CD3 - Highlights background T-lymphocytes which are an admixture of CD4 and CD8 positive T-cells	1	3.7
CD20 - Highlights B-cells		
CD68 - Positive in histiocytes		
CD138 - Positive in plasma cells		
S100 is negative		
MIB1 labeling is high around the vessels		
CD3 and CD20 highlight the mixed population of T and B-lymphocyte cells, respectively.	1	3.7
CD68 highlights the histiocytes and macrophages. GFAP highlights the reactive astrocytes.		
pNF highlights the intact axons in the areas of myelin pallor. Few bulbous aggregates pNF are present, indicating disrupted axons		
IHC for CMV, HSV, and SV40 (for JC virus) are negative.		
Diffuse glioma, IDH mutant {IDH1(R132H) positive by IHC}, NOS, WHO grade 2, and right premotor cortex. Advised FISH for 1p/19q co-deletion study.	1	3.7
GFAP - Positive in tumor cells	1	3.7
IDH1(R132H) - Positive in tumor cells		
ATRX - Retained expression in tumor cells		
p53 - Negative		
MIB1 labeling index - 4-6%		
GFAP highlights prominent reactive astrocytes.	1	3.7
No IDH1 R132H Positive or p53 positive cells are seen.		
ATRX - Retained nuclear expression		
MIB1 labels only an occasional cell.		
GFAP - Positive, highlights the reactive glial cells.	1	3.7
CD3 - Highlights the reactive T lymphocytes		
CD20 - Negative		
MIB-1 labeling: Occasional MiB1 labeled cells seen (? nature/? reactive)		
IDH1 (R 132H) Negative	1	3.7
IDH1 p.R132H - Positive	1	3.7
ATRX - Retained nuclear expression		
p53 - Negative		
Ki67 labeling - 12%		
IDH1 p.R132H - Negative	1	3.7
ATRX - Retained nuclear expression		
P53 - Negative		
Ki67 labeling index - 25%		

(Contd...)

Table 5: (Continued).

Immunohistochemistry	Count	Percentage
IDH1 p.R132H - Negative	1	3.7
ATRX - Loss of nuclear expression		
p53 - Negative		
H3K27me3 - Loss of expression		
H3K27M - Positive		
Ki67 labeling index - 15-18%		
IDH1 - Negative	1	3.7
ATRX and H3K27Me3 - Retained expression		
P53 - Positive.		
H3K27M - Negative,		
Ki67 labeling - 12-15%.		
IDH1(R132H) - Negative	1	3.7
ATRX - Equivocal		
Cytokeratin - Negative		
MIB1 labels a few scattered cells		
IDH1(R132H) - Negative	1	3.7
ATRX - Retained expression		
p53 - Focal weak positivity noted		
MIB1 Labels scattered cells		
GFAP - Positive in the cells and stroma, highlights a few hypertrophic astrocytes		
CD68 - Labels histiocytes		
IDH1(R132H) - Positive in tumor cells	1	3.7
p53 - Diffuse strong nuclear positivity in tumor cells		
IDH1R132H - Negative	1	3.7
ATRX - Retained expression		
p53 - Negative		
MIB1 labeling index - 10-12% at hotspots.		
Olig2 - Positive		
H3K27M - Negative		
H3K27me3 - Retained expression		
IDH1R132H - Positive	1	3.7
ATRX - Retained expression		
p53 - Negative		
OLIG2 Positive		
H3K27M - Negative		
LCA - Occasional interstitial cells are positive	1	3.7
CD3, CD20 - Occasional interstitial cells are positive		
GFAP - Negative		
CD68 - Occasional interstitial cells and perivascular cells are labeled		
IDH1 p.R132H - Negative		
NF-preserved in most areas, focal areas show mild disruption and axonal swellings		
Cytokeratin - Negative		
Ki-67 labeling index - Few interstitial cells are labeled		

(Contd...)

Table 5: (Continued).

Immunohistochemistry	Count	Percentage
NA	6	22.2
OLIG2 - Labels the glial cells	1	3.7
GFAP - Labels reactive hypertrophic astrocytes		
NF- Highlights preserved axons		
IDH1 p.R132H, p53 - Negative		
ATRX - Retained nuclear expression		
SV-40 - Negative		
CD68 - Labels the resting microglia		
CD3 labels T lymphocytes		
CD20 - Negative		
Ki67 labels only an occasional cell		
Same as the HPE report	1	3.7
The neoplastic lymphoid cells are LCA and CD20 positive. CD3 highlights the reactive T-lymphocytes.	2	7.4
Total	27	100.0

NF: Neurofilament, GFAP: Glial fibrillary acidic protein, IDH 1: Isocitrate dehydrogenase 1, HPE: Histopathological examination, WHO: World Health Organization, LCA: Leukocyte common antigen

Table 6: MIB index (n=27).

MIB index	Count	Percentage
-	17	63.0
0.03	1	3.7
0.04	1	3.7
10–12%	1	3.7
4–5%	1	3.7
4–6%	1	3.7
MIB1 labeling is high around the vessels	1	3.7
NA	3	11.1
Occasional cells	1	3.7
Total	27	100.0

MIB: antibody Mindbomb Homolog-1, NA: Not applicable

perilesional edema was seen in 2% of cases. None of the cases needed an open procedure after the biopsy.

DISCUSSION

The introduction of STB has proved critical in arriving at tissue diagnosis for various brain pathologies, including neoplasm. Studies showed no statistically significant differences in the accuracy and retrieval of diagnostic tissue between frame-based and frameless methods. Preoperative planning is based on careful selection of the particular imaging sequence from CT or MRI, in which the target is better visualized, mainly in contrast sequences. Sampling errors are of particular concern in the case of contrast non-enhancing targets/lesions. Advanced imaging modalities such as perfusion sequences, PET, and magnetic resonance spectroscopy are used as adjuncts

for better visualization of such targets/lesions reported high diagnostic yield in small studies ($n = 12-32$) by few authors.^[12]

There are several factors to discuss when considering a new method for targeting. One important aspect is the diagnostic yield, which is influenced by the patient's age, volume of the biopsied lesion, and histopathology.^[11] In a recent meta-analysis, among the 15 studies included, 10 of them accounted for the size of the lesion. Over 90% of the biopsied lesions were observed to be larger than 1 cm in diameter. Therefore, the results of the meta-analysis may not apply to lesions smaller than 1 cm. In such cases, many neurosurgeons prefer using frame-based biopsy techniques. However, the impact of the number of biopsy specimens on the diagnostic yield cannot be adequately analyzed due to limited data, as only four studies have provided information on this aspect.

Another factor is morbidity and mortality; it is known that the risk is influenced by the location of the lesion, with higher risks associated with lesions situated in deep gray matter, brainstem, and eloquent regions. Unfortunately, most identified studies did not provide information on lesion location. Some surgeons opt for frame-based approaches when dealing with lesions in the pineal region, brainstem, basal ganglia, thalamus, posterior fossa, and deep perivascular regions, as frame-based systems offer more precise stereotactic guidance.^[3] Furthermore, it is generally believed that the number of biopsy specimens taken can affect the risk of complications. However, more data are needed to quantify the contribution of the number of biopsy samples to the observed morbidity and mortality rates in this study. Finally, certain intracranial lesions have an increased risk of hemorrhage. Patients with cancer and intracranial lesions who have recently undergone chemotherapy or have a hematologic malignancy may have thrombocytopenia or other forms of coagulopathy, which further increases the risk. Fortunately, our targeting system does not add to any of these complications while providing a 92.59% diagnostic accuracy, comparable to previously reported studies.^[6]

In terms of procedure duration, our study supported the notion that indirect evidence-targeted biopsy offers time savings compared to the large amount of time needed for higher-order imaging after frame fixation in other methods. However, the time saved may vary depending on institutional workflow, including travel time to and from imaging units and surgeon preference. It is worth noting that although time savings are essential, transporting patients under general anesthesia has its risks. Therefore, it is crucial to consider these factors when interpreting our results.

Limitations

We acknowledge certain limitations to our research. First, some of the other parameters (age, size of the lesion, lesion location, etc.) may be predictive of the location of the lesion, which we have not considered. Further research focused on the other parameters may demonstrate differences not

shown in our study. Second, indirect targeting may only be applicable in some cases due to the small numbers. A prospective evaluation may reveal the advantages and disadvantages of our suggested target selection technique.

CONCLUSION

Indirect targeting is a safe and intuitive method for the biopsy of non-enhancing lesions. This eliminates the need for higher-order imaging and, thus, saves time and money spent while not compromising diagnostic accuracy and safety. Due consideration is to be given to the findings observed in non-contrast CT scans of the head as indirect evidence of target selection while performing frame-based STB of contrast non-enhancing lesions. A more extensive series with a comparison arm of direct targeting comparing diagnostic accuracy and safety will be the next step in our series.

Ethical approval

The Institutional Review Board approval is not required as the study was retrospective in nature.

Declaration of patient consent

Patients' consent not required as patients' identities were not disclosed or compromised.

Financial support and sponsorship

Nil.

Conflicts of interest

There are no conflicts of interest.

Use of artificial intelligence (AI)-assisted technology for manuscript preparation

The authors confirm that there was no use of artificial intelligence (AI)-assisted technology for assisting in the writing or editing of the manuscript, and no images were manipulated using AI.

REFERENCES

1. Akshulakov SK, Kerimbayev TT, Biryuchkov MY, Urunbayev YA, Farhadi DS, Byvaltsev VA. Current trends

for improving safety of stereotactic brain biopsies: Advanced optical methods for vessel avoidance and tumor detection. *Front Oncol* 2019;9:947.

2. Chernov MF, Muragaki Y, Ochiai T, Taira T, Ono Y, Usukura M, *et al.* Spectroscopy-supported frame-based image-guided stereotactic biopsy of parenchymal brain lesions: Comparative evaluation of diagnostic yield and diagnostic accuracy. *Clin Neurol Neurosurg* 2009;111:527-35.
3. Dhawan S, He Y, Bartek J Jr, Alattar AA, Chen CC. Comparison of frame-based versus frameless intracranial stereotactic biopsy: Systematic review and meta-analysis. *World Neurosurg* 2019;127:607-16.e4.
4. Eigenbrod S, Trabold R, Brucker D, Eros C, Egensperger R, La Fougere C, *et al.* Molecular stereotactic biopsy technique improves diagnostic accuracy and enables personalized treatment strategies in glioma patients. *Acta Neurochir (Wien)* 2014;156:1427-40.
5. Farahmand D, Keil F, Gohring M, Dinc N, Seifert V, Marquardt G, *et al.* Prognostic risk factors for postoperative hemorrhage in stereotactic biopsies of lesions in the basal ganglia. *Clin Neurol Neurosurg* 2018;174:180-4.
6. He Z, Zhu CX, Chan DT, Cheung TC, Ng HK, Mok VC, *et al.* Diagnostic accuracy and field for improvement of frameless stereotactic brain biopsy: A focus on nondiagnostic cases. *J Neurol Surg A Cent Eur Neurosurg* 2024;85:48-61.
7. Hemm S, Rigau V, Chevalier J, Picot MC, Bauchet L, El Fertit H, *et al.* Stereotactic coregistration of 201Tl SPECT and MRI applied to brain tumor biopsies. *J Nucl Med* 2005;46:1151-7.
8. Kesserwan MA, Shakil H, Lannon M, McGinn R, Banfield L, Nath S, *et al.* Frame-based versus frameless stereotactic brain biopsies: A systematic review and meta-analysis. *Surg Neurol Int* 2021;12:52.
9. Pirotte B, Goldman S, Massager N, David P, Wikler D, Vandesteene A, *et al.* Comparison of 18F-FDG and 11C-methionine for PET-guided stereotactic brain biopsy of gliomas. *J Nucl Med* 2004;45:1293-8.
10. Pirotte BJ, Lubansu A, Massager N, Wikler D, Goldman S, Levivier M. Results of positron emission tomography guidance and reassessment of the utility of and indications for stereotactic biopsy in children with infiltrative brainstem tumors. *J Neurosurg* 2007;107(5 Suppl):392-9.
11. Tsermoulas G, Mukerji N, Borah AJ, Mitchell P, Ross N. Factors affecting diagnostic yield in needle biopsy for brain lesions. *Br J Neurosurg* 2013;27:207-11.
12. Winn HR. Youmans and Winn neurological surgery e-book. Vol. 4. Netherlands: Elsevier Health Sciences; 2022.

How to cite this article: Lingaraju TS, Prabhuraj AR, Nandeesh BN, Saini J, Pruthi N. Computed tomography-guided frame-based stereotactic brain biopsy of non-enhancing lesions using indirect evidence of target selection, technical consideration, and early clinical experience. *Surg Neurol Int.* 2024;15:286. doi: 10.25259/SNI_187_2024

Disclaimer

The views and opinions expressed in this article are those of the authors and do not necessarily reflect the official policy or position of the Journal or its management. The information contained in this article should not be considered to be medical advice; patients should consult their own physicians for advice as to their specific medical needs.